Tribology Letters, Vol. 19, No. 1, May 2005 (© 2005)
DOI: 10.1007/s11249-004-4261-2

Reduction of adhesion and friction of silicon oxide surface in the presence of *n*-propanol vapor in the gas phase

K. Strawhecker[a], D.B. Asay[a], J. McKinney[c] and S.H. Kim[a,b,*]

[a]*Department of Chemical Engineering, The Pennsylvania State University, University Park, PA 16802, USA*
[b]*Materials Research Institute, The Pennsylvania State University, University Park, PA 16802, USA*
[c]*REU Student from Department of Chemical Engineering, University of South Carolina, USA*

Received 15 April 2004; accepted 4 July 2004

The equilibrium adsorption of gas phase alcohol molecules has been proposed as a new means of in-use anti-stiction and lubrication for MEMS devices. Adhesion and friction of silicon oxide surfaces as a function of *n*-propanol vapor pressure in the ambient gas were invesitigated using atomic force microscopy. As the vapor pressure increases, the adsorbed *n*-propanol layer thickness increases. The adhesion and friction significantly decrease with very little addition of *n*-propanol vapor.

KEY WORDS: MEMS, lubrication, adhesion, friction, alcohol, adsorption

1. Introduction

One of the main challenges preventing wide scale use of microelectromechanical system (MEMS) devices is obtaining fully conformal, continuously replenishing, low-friction coating layers on the device surface that will not interfere with the device function or performance [1]. Most approaches published in the MEMS lubrication literature rely on solid phase lubrication utilizing hard coatings such as diamond-like carbon [2,3], carbides [4,5], nitrides [6] and oxides[7] or hydrophobic organic coatings such as self-assembled monolayers (SAM) [8,9]. Although these approaches have made significant improvements in conformal coating and reduction of friction as well as reduced wear in laboratory tests, they have technical limitations relating to their durability. Solid lubricant coatings and SAMs have been shown to wear off during MEMS operation [10,11]. What is absent in these thin film lubrication systems is the capability for continuous replenishment of the lubricating layer. In fact, the continuous replenishment of lubricating layers has been the key feature of the conventional lubrication approaches using viscous liquids. Unfortunately, the viscous nature of the liquid lubricant causes power dissipation making their usage in MEMS devices undesirable.

This study explores the use of equilibrium adsorption of gas-phase lubrication molecules on the solid substrate as a new means of MEMS device lubrication. The surface of all inorganic materials exposed to ambient (humid) air is always covered with a thin layer of water adsorbed from the gas phase [12,13]. The thickness of the adsorbed water layer varies with the humidity and surface chemistry [14]. This water layer has been shown to reduce wear in MEMS operation [15]. However, the high surface tension of the water film can cause an in-use stiction problem. The gas-phase lubrication concept discussed in this paper employs the same equilibrium adsorption principle as the water adsorption in humid environments. The difference is that our approach utilizes a ‘surfactant-like’ molecule that can provide low adhesion and good lubrication.

This gas-phase lubrication approach eliminates the power dissipation problem of the liquid-phase approach without sacrificing advantages. The adsorption of gas-phase lubricant molecules will occur on all surfaces exposed to the gas phase molecules. The coverage of the surface depends on the adsorption isotherm, which is a function of pressure of the overlying gas and surface chemistry of the substrate. This surface coverage will readily occur even on so-called ‘buried’ interfaces as long as the clearance of moving parts is larger than the mean free path of the adsorbate molecules. Since the surface lubricant molecules are in equilibrium with the gas phase, the lubricant layer will be continuously replenished. Because there is no bulk liquid between moving parts, there is little resistance to the motion of MEMS parts such as viscous drag. Another important feature of gas-phase lubrication is that it can be employed independently or in conjunction with other surface modifications [16].

Simple alcohol molecules can be used as a gas-phase lubricant for MEMS devices. Small alcohol molecules have vapor pressures high enough for gas-phase mass transport. Depending on the operation temperature range, different types of alcohol can be chosen. For low temperature operation, small alcohol molecules would

*To whom correspondence should be addressed.
E-mail: shkim@engr.psu.edu

1023-8883/05/0500–0017/0 © 2005 Springer Science+Business Media, Inc.

be appropriate (for example, the freezing temperature of ethanol = −117 °C). Long alkyl-chain alcohols such as *n*-octanol (boiling temperature = 196 °C) would be suitable for high temperature operation. The amphiphilic nature of the alcohol molecule provides unique properties. The hydrophilic OH group provides good adsorptivity [17] and solubility into water that may be present at the device surface in ambient conditions. The hydrophobic nature of the alkyl chain induces segregation of the alcohol molecules at the air–water interface, forming a monolayer of alcohol with alkyl groups pointing toward the air [18]. The structural ordering at the air–water interface renders a low surface tension even at a very low alcohol concentration in the solution[19] which resolves the in-use stiction problem. In liquid phase lubrication studies, alcohols have shown good lubrication and anti-wear properties for silicon oxide and silicon nitride surfaces [20]. The presence of a few layers of alcohol at the MEMS surface does not interfere with optical reflection or electrical contact of devices, which is an important aspect for MEMS device operations.

In this paper, we investigate the effect of the equilibrium adsorption of *n*-propanol at room temperature on the adhesion and friction of silicon oxide surfaces using atomic force microscopy (AFM). When the clean silicon oxide surfaces are exposed to the *n*-propanol containing gas, it is found that their adhesion and friction decreases immediately even at low *n*-propanol partial pressure. This result is much different and significant compared to the effect of the water adsorption that increases adhesion and friction of the silicon oxide surfaces.

2. Experimental

Figure 1 shows the schematics of the apparatus used for adhesion and friction measurement as a function of the gas-phase alcohol concentration. The gas composition is controlled by adjusting the ratio of dry argon flowrate to the saturated *n*-propanol/argon flowrate. The mixture of argon and saturated *n*-propanol vapor is produced by flowing dry argon gas through a heated bubbler containing *n*-propanol (EM Science, 99.95%) and a condenser held at the experimental temperature. The purpose of the condenser is to remove any super-saturated alcohol vapor from the argon gas flow, leaving only argon with saturated alcohol vapor at the experimental temperature. This eliminates bulk liquid condensation on the experimental surfaces and apparatus. The AFM experiments performed in this work were done using a Molecular Imaging PicoSPM head and a RHK Technology controller. All measurements were made at room temperature. This temperature was maintained throughout the experiment. The substrate was cleaned with a piranha solution (H_2SO_4/30%–H_2O_2 = 70/30) followed by UV-ozone cleaning and

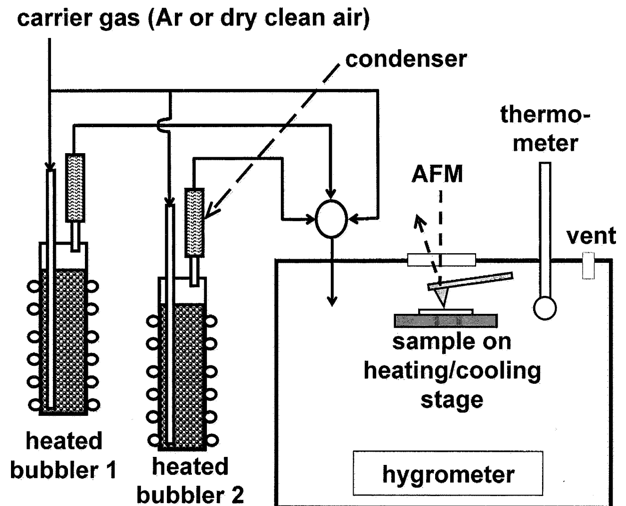

Figure 1. Schematic diagram of the gas-handling system and the environment-controlled AFM chamber. The *n*-propanol partial pressure is controlled by varying the ratio of dry Ar and *n*-propanol saturated Ar gas flow rates. The *n*-propanol saturated Ar gas stream is generated by flowing Ar through a heated bubble followed by a condensor held at room temperature (which converts the vapor from super-saturated to saturated at the experimental temperature, thereby avoiding bulk condensation of the alcohol in the experimental system).

heating to 300 °C. A silicon tip (force constant = 2.2 N/m and 4.5 N/m; nominal tip diameter = 20 nm) covered with a native oxide layer was cleaned with the UV-ozone treatment. The sample and tip were maintained in the environmental chamber during the AFM experiment. Adhesion force was determined from the pull-off point of the force–distance (f–d) curve. Friction force was determined from the lateral force hyteresis in the left and right scans of the contact mode operation. In order to minimize experimental artifacts due to uncertainty in tip diameter and AFM tip aligning, the measured adhesion and friction forces were normalized to the initial adhesion and friction force values measured with dry argon flowing previous to each experiment.

The adsorption isotherm of *n*-propanol was measured using a quartz crystal microbalance (QCM) and attenuated total reflection infrared (ATR-IR) spectroscopy, while varying the partial pressures of *n*-propanol in dry Argon. The experiment was performed at room temperature. The QCM was directly mounted in the environmental chamber. In QCM monitoring, the adsorbed film thickness was calculated from the Sauerbrey equation using the observed frequency decrease and the density of *n*-propanol liquid [21]. The vent gas from the environment-controlled chamber was passed through a sealed Ge ATR cell. In ATR-IR monitoring, the film thickness was calculated by comparing the observed peak intensity with the ATR-IR spectra of *n*-propanol liquid and the effective penetration depth of the ATR-IR experiment at a given wavelength [22]. The QCM and

ATR-IR experiments were carried out separately from the AFM measurements.

3. Results and discussion

The active control of the *n*-propanol partial pressure was confirmed by monitoring the adsorption isotherm characteristics of *n*-propanol. Figure 2 shows the thickness of the *n*-propanol layer, measured with two different techniques, at various *n*-propanol relative partial pressures. The inset shows the C–H and O–H stretching vibration peaks of the adsorbed *n*-propanol layer, which are in agreement with those of liquid *n*-propanol. The observation of the bulk condensation (steep rise in thickness, especially in the QCM data) when the chamber is completely flushed with the gas from the *n*-propanol bubbler confirms that the gas flow system used in this experiment does generate the saturation vapor pressure. The reason that the thickness calculated from the ATR-IR data is lower than that from the QCM data might be due to slight temperature difference between the environment-controlled chamber and the ATR-IR unit. The observed trend of the *n*-propanol film thickness as a function of partial pressure is consistent with the general characteristic of the alcohol adsorption isotherm observed for other systems [23–25]. However, it should be noted that the thickness data shown in figure 2 are measured for gold (in QCM) and Ge (in ATR-IR) substrates. The actual *n*-propanol thickness on the clean, hydrophilic silicon oxide surface would be slightly larger than those on gold and Ge surfaces [25].

The *n*-propanol adsorption from the gas phase significantly decreases the adhesion force between the silicon oxide surfaces measured with AFM. Figure 3 reports the pull-off force measured with a single tip (2.2 N/m) at various *n*-propanol partial pressure in the gas phase. The adhesion force drops by 40%, compared to the dry Ar case, upon increase of the *n*-propanol partial pressure from zero to 10% and then decreases slowly upon further increase of the *n*-propanol partial pressure. The large decrease at only 10% of the *n*-propanol saturation partial pressure indicates that a few monolayer thick *n*-propanol film is sufficient to reduce the adhesion between the silicon oxide surfaces. This behavior is in sharp contrast to the relationship between the adhesion force and the water adsorption isotherm. In the case of water, the adhesion force increases several fold when the relative humidity increases from zero to 50% [26,27]. We have observed the same increase trend upon increase of humidity in our system [data not shown].

This difference could be attributed to the amphiphilic nature of the alcohol. In the case of water, the free OH groups at the surface of the adsorbed water layer on the substrate can form hydrogen bonding with their counterparts on the AFM tip, which will cause high adhesion force. In the case of *n*-propanol, the OH groups have strong interaction with the substrate surface [28] and the hydrophobic propyl groups are likely to be exposed at the air interface of the adsorbed layer [18]. In this structure, the hydrogen bonding interaction between two *n*-propanol layers adsorbed on the substrate and the tip will be very small, leading to much smaller adhesion force.

The *n*-propanol layer in equilibrium with the gas phase reduces the friction between the silicon oxide substrate and AFM tip. Figure 4 plots the lateral force signal (which is directly proportional to the friction force) versus applied normal load at various *n*-propanol partial pressures. All of the data in figure 4 were acquired with a single tip (4.5 N/m) without disturbing the

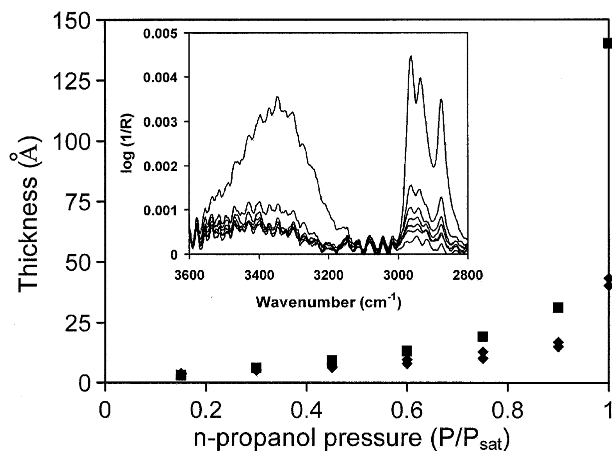

Figure 2. Thickness of the adsorbed *n*-propanol layer measured with (■) QCM and (♦) ATR-IR as a function of *n*-propanol partial pressure. It should be noted that the QCM measures the thickness on a gold surface and the ATR-IR measures that on a Ge surface. The inset shows the C–H and O–H stretching region of the *n*-propanol adsorbed on the Ge-ATR crystal. The saturation vapor pressure on *n*-propanol is 21.2 Torr at room temperature.

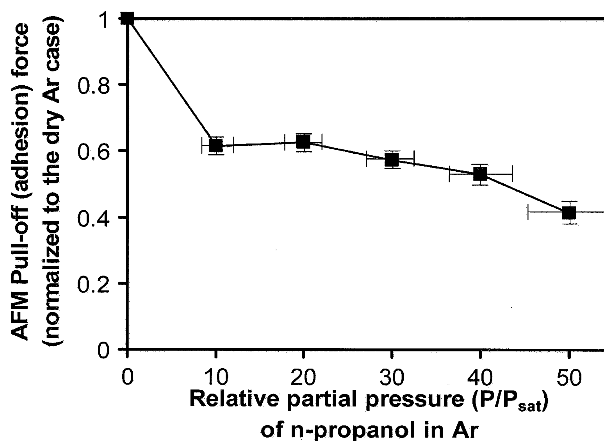

Figure 3. Pull-off force (adhesion force) measured with AFM as a function of n-propanol partial pressure. The data are normalized to the dry Ar case which is measured before the *n*-propanol exposure. Data are acquired with a single tip (2.2 N/m).

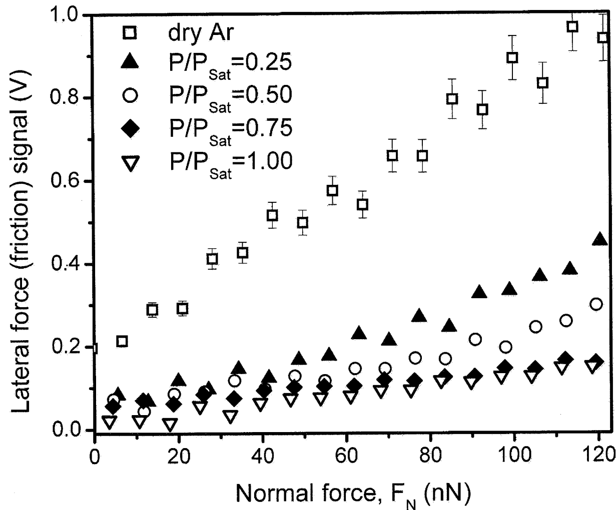

Figure 4. Lateral force (friction force) measured with AFM as a function of *n*-propanol partial pressure. The lateral force signal was recorded as the normal load decreased from 100 to 0 nN. Data are acquired with a single tip (4.5 N/m).

cantilever, laser, or detector alignments, while the *n*-propanol partial pressure was increased from zero to its saturation value. As in the adhesion case, the friction force significantly decreases upon initial increase of *n*-propanol vapor pressure from 0 to 25% of the saturation pressure. Further increase in the *n*-propanol vapor pressure results in a gradual decrease in friction force, which seems to level off at the higher partial pressures of 75 and 100%. This sharp decrease of the friction force upon introduction of *n*-propanol vapor into the gas phase is very promising for MEMS lubrication applications. In the case of water, the friction force at low humidity is reported to be higher than that at the dry condition [27,29,30]. These results indicate that unlike the water adsorption, the *n*-propanol adsorption can be used for lubrication of the silicon oxide surface.

Figure 5 displays the slope and *y*-intercept of the friction-versus-load curve (of figure 4) as a function of the *n*-propanol partial pressure. The slope corresponds to the friction coefficient and the *y*-intercept defines the adhesion-induced friction at the zero applied normal force. It illustrates that the formation of the *n*-propanol layer on the silicon oxide surface reduces the friction coefficient significantly. It should be noted that the trend of the friction force change is very close to that of the adhesion force (figures 3 and 5). Both friction and adhesion forces show initial large decrease upon introduction of *n*-propanol vapor followed by a small decrease upon further increase of *n*-propanol vapor. The decrease of adhesion force (figure 3) results in lower friction force at zero normal load (figure 5(b)), which is consistent with the JKR theory [31] and shows that at low loads the frictional force varies with load in proportion to the contact area that is in turn a function of adhesion force. The decrease of the friction coefficient (figure 5(a)) must be related to the lubrication effect of the adsorbed *n*-propanol molecules.

The friction coefficient and the friction force at zero normal load were also measured, while the *n*-propanol partial pressure was decreasing from the saturation to zero and these data are also shown in figure 5. It should be noted that upon decrease of the *n*-propanol partial pressure from the saturation vapor pressure to zero, the friction coefficient and the zero-load friction force increase close to – *but not much higher than* – its initial values. If the AFM tip became worn and dull during the friction force measurement, the zero-load friction force would increase to a value higher than the initial value since the tip contact area would have increased [31]. This is not the case in our experiment, and indicates that there is little or no tip wear during the contact mode scan in the *n*-propanol vapor environment. In a scanning electron microscope experiment, the tip diameter of a Si tip (coated with a native oxide layer) is found to be

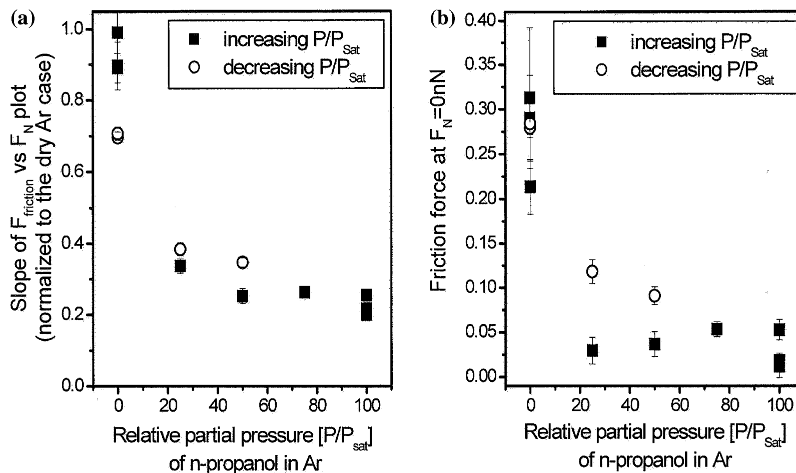

Figure 5. (a) Slope and (b) *y*-intercept of the friction-versus-load curve as a function of *n*-propanol partial pressure. Filled squares are data taken at increasingly larger constant partial pressures, and open circles are data taken at decreasingly smaller constant partial pressures.

less than 50 nm after the wear test in the saturated *n*-propanol vapor, while it is increased to ~350 nm after the wear test at the same applied load (135 nN) in the humid air environment [32]. The lower friction coefficient and lower zero-load friction force upon returning to dry Ar environments might be an indication of some residual *n*-propanol molecules strongly bound to silicon oxide surfaces. If *n*-propoxide groups are formed, these would not be removed from the surface by simply lowering the *n*-propanol vapor pressure at room temperature.

Further experiments have shown that the results discussed here are not limited to *n*-propanol, but that other linear alcohols (ethanol, butanol, and pentanol) also produce similar results [32]. A deeper understanding of the process and the conditions necessary for the minimization of adhesion, friction, and wear of the device surfaces should take into account the surface chemistry of the adsorbed molecules as well as the equilibrium adsorption isotherm, which will be the subject of future publications. The utility of this work lies in the application of *n*-propanol (or, in general, any lubricant molecules which will easily adsorb on substrates from the gas phase) to the surfaces of devices where the moving parts have a large surface-to-volume ratio. This can easily be done for MEMS devices operated in an environment-controlled system. In the case of hermetically sealed MEMS devices [33], one can achieve the vapor phase lubrication by enclosing a small amount of liquid or a material that can emit lubricant vapor (opposite to a 'getter' demonstrated in ref. [34]).

4. Conclusions

The AFM study of the effect of the *n*-propanol vapor in the gas phase on the adhesion and friction of silicon oxide surfaces shows very promising results. Unlike the water vapor exposure (humid air), the adhesion force as well as the friction force and coefficient decrease immediately upon introduction of *n*-propanol vapor into the gas above the substrate surface. This phenomenon can be used to develop a gas-phase anti-stiction and lubrication process suitable for MEMS device operation.

Acknowledgments

This work is supported by Penn State Start-up Funds and National Science Foundation (Grant No. CMS-0408369). The summer REU program for J. P. McKinney was supported by Penn State Materials Research Institute and the Penn State MRSEC under NSF Grant DMR 0213623.

References

[1] S.M. Hsu and Z.C. Ying, *Nanotribology Critical Assessment and Research Needs* (Kluwer Academic Publishers, Boston, 2003).
[2] A.R. Krauss, O. Auciello, D.M. Gruen, A. Jayatissa, A. Sumant, J. Tucek, D.C. Mancini, N. Moldovan, A. Erdemir, D. Ersoy, M.N. Gardo, H.G. Busmann, E.M. Meyer and M.Q. Ding, Diamond and Related Materials 10 (2001) 1952.
[3] S. Sundararajan and B. Bhushan, Wear 225 (1999) 678.
[4] C.R. Stoldt, C. Carraro, W.R. Ashurst, D. Gao, R.T. Howe and R. Maboudian, Sensors Actuators A-Phys. 97 (2002) 410.
[5] S. Sundararajan and B. Bhushan, Wear 217 (1998) 251.
[6] D.F. Wang and K. Kato, Tribol. Int. 34 (2001) 407.
[7] T.M. Mayer, J.W. Elam, S.M. George, P.G. Kotula and R.S. Goeke, Appl. Phys. Lett. 82 (2003) 2883.
[8] W.R. Ashurst, C. Yau, C. Carraro, C. Lee, G.J. Kluth, R.T. Howe and R. Maboudian, Sensors Actuators A 91 (2001) 239.
[9] S.T. Patton, W.D. Cowan, K.C. Eapen and J.S. Zabinski, Tribol. Lett. 9 (2000) 199.
[10] S. Sundararajan and B. Bhushan, Wear 225 (1999) 678.
[11] K.C. Eapen, S.T. Patton and J.S. Zabinski, Tribol. Lett. 12 (2002) 35.
[12] A. Opitz, S.I.-U. Ahmed, J.A. Schaefer and M. Scherge, Surf. Sci 504 (2002) 199.
[13] R. Maboudian, W.R. Ashurst and C. Carraro, Tribol. Lett. 12 (2002) 95.
[14] R.M. Pashley and J.A. Kitchener, J. Colloid Interface Sci. 71 (1979) 491.
[15] S.T. Patton and J.S. Zabinski, Tribol. Int. 35 (2002) 373.
[16] H. Yoshizawa, Y.-L. Chen and J. Israelachvili, J. Phys. Chem. 97 (1993) 4128.
[17] D.J. Donaldson and D. Anderson, J. Phys. Chem. A 103 (1999) 871.
[18] P.B. Miranda, V. Pflumio, H. Saijo and Y.R. Shen, J. Am. Chem. Soc. 120 (1998) 12092.
[19] P. Lavi and A. Marmur, J. Colloid Interface Sci. 230 (2000) 107.
[20] R.S. Gates and S.M. Hsu, Tribol. Trans. 38 (1995) 607.
[21] M. Rodahl and B. Kasemo, Sensors Acutators A 54 (1996) 448.
[22] M.W. Urban, *Attenuated Total Reflectance Spectroscopy of Polymers American Chemical Society* (Washington DC, 1996) 37.
[23] M.J. Adams, B.J. Briscoe, J.Y.C. Law, P.F. Luckham and D.R. Williams, Langmuir 17 (2001) 6953.
[24] S. Kittaka, T. Umezu, H. Ogawa, H. Maegawa and T. Takenaka, Langmuir 14 (1998) 832.
[25] M. Nagao and T. Morimoto, J. Phys. Chem. 84 (1980) 2054.
[26] M. He, A.S. Blum, D.E. Aston, C. Buenviaje, R.N. Overney and R. Luginbuhl, J. Chem. Phys. 114 (2001) 1355.
[27] L. Qian, F. Tian and X. Xiao, Tribol. Lett. 15 (2003) 169.
[28] M. Mizukami, M. Moteki and K. Kurihara, J. Am. Chem. Soc. 124 (2002) 12889.
[29] B. Bhushan and H. Liu, Phys. Rev. B 63 (2001) 245412.
[30] M. Binggeli and C.M. Mate, Appl. Phys. Lett. 65 (1994) 415.
[31] R.W. Carpick, N. Agrait, D.F. Ogletree and M. Salmeron, J. Vac. Sci. Technol. B 14 (1996) 1289.
[32] K. Strawhecker, D. Asay and S.H. Kim, Marcel Dekker Encyclopaedia of Chemical Processing (in press).
[33] M. Karpman, US Patent 6,441,481 (2002).
[34] Y. Jin, Z. Wang, L. Zhao, P.C. Lim, J. Wei and C.K. Wong, J. Micromech. Microeng. 14 (2004) 687.